Sustainable Energy Technologies and Assessments 50 (2022) 101813

Contents lists available at ScienceDirect

Sustainable Energy Technologies and Assessments

journal homepage: www.elsevier.com/locate/seta

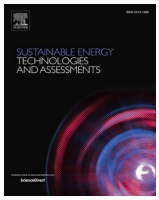

A lab-scale study on thermal performance enhancement of phase change material containing multi-wall carbon nanotubes for buildings free-cooling

Mahdi Kazemi, Ali Kianifar *, Hamid Niazmand

Department of Mechanical Engineering, Ferdowsi University of Mashhad, Mashhad, Iran

ARTICLE INFO

Keywords:
Encapsulation
Building
Heat exchanger
Melting
Solidification

ABSTRACT

The aim of this research was to experimentally investigate feasibility of using phase change material (PCM) to fabricate an air-PCM heat exchanger to be used in buildings in order to have an effective thermal management as well as enhanced energy performance. RT22HC was selected and encapsulated in the heat exchanger. Due to low thermal conductivity of PCM, multi-wall carbon nanotube (MWCNT) nanoparticles were dispersed into the PCM to compensate this shortage. First, experiments with pure PCM for three successive days had a maximum outlet air temperature of 31.76 °C. As stated, nano-PCM with three different mass fractions (0.1%, 0.2%, and 0.5% wt.) reduced the melting and solidification time compared to the pure PCM. By calculating the absorbed heat by air, 24.1% more heat was charged in encapsulations in the case nano-PCM 0.5% wt. compared to the pure PCM. By investigating the time–temperature behavior of four types of PCMs in solidification, it was observed that rising the nanoparticles concentration decreased the two-phase duration and increased two-phase temperature. Moreover, with the aid of an IR camera, during sensible heating the encapsulation's wall temperature is near the nano-PCM temperature, whereas when latent heating, this difference is much more (@T_{PCM} = 20.00: $T_{encapsulation}$ = 21.41; (@ T_{PCM} = 21.15: $T_{encapsulation}$ = 23.17).

Introduction

The COVID-19 pandemic stay-at-home policies have made people spend more time at their homes and this has resulted in more energy usage. More energy consumption increases greenhouse gases emissions, which is one of the most critical economic challenges [1]. Furthermore, many environmental and human health concerns arise by further using of non-renewable sources [2]. Because of the sustainability of renewable energies such as solar, wind, biogas, and geothermal; these energies are considered suitable alternatives for fossil fuels. Using thermal energy storage (TES), due to the intermittent nature of solar energy, is a different way to employ the thermal energy of the sun [3]. Subsequent operations are needed to transform the stored energy to desired forms. The latent heat thermal energy storage systems (LHTES) have higher storage density and temperature stability than the sensible heat storage, making it an excellent method for energy storage [4]. Phase change materials (PCMs) are employed in LHTES. During the melting and solidification processes, the PCMs can store and deliver a significant amount of energy. The LHTES are applicable in many fields such as cooling devices (PCM based round pin–fin heat sinks [5], paraffin-based heat sink [6], PCM-based thermoelectric energy-harvesting [7]), solar systems (concentrated photovoltaic using PCM [8], solar collector [9], solar distillation system using PCM [10], concentrated photovoltaic solar cells with PCM [11]), free cooling and heating of buildings (clean energy storage using porous foam [12], PCMs for building façade applications [13], PCMs and nano-PCMs melting and freezing [14], PCM triple heat exchanger [15], PCM Trombe wall in building [16], PCM nano-emulsion in a heat exchanger [17]), thermal inertia, and thermal protection [18,19].

Phase change materials fall into three different groups: organic, inorganic, and eutectics [20,21]. One of the most used organic PCMs is Paraffin. That is because of its desirable features and properties like large latent heat, consistent melting properties, slight volume change when solidification /melting, low cost, chemical stability, non-corrosiveness, and non-toxicity [6,22]. Due to the mentioned advantages of paraffin, they can be packed or encapsulated into building structures. Since no conventional energy is required, the system is called passive [23,24]. In free cooling, the PCMs ,which can be placed into buildings, release heat during solidification process (nighttime) and absorb heat during melting process (daytime), causing a lower heat flow from outdoors to indoors [25]. During winter, the system can also be

* Corresponding author.
E-mail address: a-kiani@ferdowsi.um.ac.ir (A. Kianifar).

https://doi.org/10.1016/j.seta.2021.101813
Received 13 April 2021; Received in revised form 7 September 2021; Accepted 7 September 2021

Nomenclature

C_p	Specific heat (J/kg. K)
Q	Rate of heat transfer (W)
$\dot{m}$	Flow rate (kg/s)
k	Thermal conductivity (W/m. K)
h	Enthalpy (J/kg)
l	Thickness (m)
A	Cross section area (m^2)
$\dot{E}$	Energy rate (W)
R	Thermal Resistance (^oC/W)
T	Temperature (K)

Subscripts

env	environment
w	wood
e	exit
out	outlet
th	Thermal
rep	repetition
i	isolation
in	inlet

Abbreviations

PCM	Phase change material
RT	Rubitherm
HC	High capacity
MWCNT	Multi-wall carbon nanotube

used for heating by utilizing solar energy during the day. In passive methods, the stored heat or cold is automatically released when indoor or outdoor temperatures rise or fall beyond the melting point of PCM [26].

It should be noted that PCM has a low thermal conductivity which slows the solidification and melting processes and limits its applications. One of the ways to improve its thermal conductivity is adding nano-sized materials [27–29]. Sheikholeslami and Mahian [30] studied the enhancement of PCM solidification using CuO nanoparticles and applying an external magnetic field. They modeled solidification processes using finite element method. The influence of some parameters on charging time was assessed such as: nanoparticles' concentration, Rayleigh number, and Lorentz force intensification. The time of solidification period decreased up to 23.5% if the Hartmann number rises from 0 to 10. Furthermore, adding nanoparticles up to 4% causes 14% reduction in the solidification period.

Santos et al. [31] experimentally evaluated the thermal performance of panels when encapsulating phase change material (PCM) and incorporating within PCM-air heat exchanger system. New design of the panels enables the system to carry 17.5 kg more PCM than the first design which also increases the solidifying and melting time. For the two thermal battery designs, using new design compared to the first design leads to 100% and 70% increase in the melting and solidifying time, respectively. Iten et al. [23] reviewed the applications of air-PCM thermal energy storage studies and technologies for the free cooling and heating of buildings. They mentioned that for extreme climates, passive techniques, e.g. use of PCMs in the buildings, because of the difficulty of exchanging high rates of heat is unsuitable. Thus, to meet the demand, active techniques are adopted for extreme climates. Providing opportunities to decrease photovoltaic (PV) panel temperature and increase overall efficiency using building integrated photovoltaic (BIPV) coupled with PCMs (BIPV/PCM) is performed by Kant et al. [32]. They simulated a setup to study the effects of different BIPV design parameters such as BIPV height, air gap between BIPV/PCM and wall, PCM thickness, and air mass flow rate on the maximum PV panel temperature, the power production by PV, and the exergy extracted by the air. Three different PCMs are employed to maximize the total energy from PV and extracted heat using Taguchi method. The optimum values of design parameters are PCM thickness of 0.04 m, BIPV height of 3 m, air gap of 0.08 m, and air flow rate of 0.18 kg/s. Osegui et al. [33] studied inverse method to estimate air flow rate during free cooling using PCM-air heat exchanger used to shave the peak load for the cooling system and decrease energy ventilation consumption. The numerical results show the robustness and consistency of their method.

Energy consumption can significantly decrease by thermal energy storage units and they can enhance the employment of renewable energy sources. From the literature, it is evident that utilization of PCMs in buildings structure affects the inside temperature. Various studies have been focused on thermal management of heat exchangers using PCM. In current paper, a PCM-based heat exchanger is fabricated. Dispersing multi-wall carbon nanotube powders in the PCM is well investigated. The utilized heat exchanger can be applied to reduce the heating load needed during the nighttime for the room as well as to reduce the cooling load required when daytime. The effect of nanoparticles concentration and inlet temperature on heating and cooling heat exchanger performance and encapsulations temperature are also investigated. The time- temperature behavior of different cases during cooling and heating processes is accomplished. Temperature of encapsulation using an IR camera has then proceeded.

Experimental section

Materials and properties

PCM is a heat storage material utilizing the processes of phase change between liquid and solid (melting and congealing) to release and store large amount of thermal energy at closely constant temperature. The PCM substance Rubitherm 22℃ High Capacity (RT22HC) is purchased. RT22HC is a non-toxic organic PCM with a high capacity. Its melting temperature lies between 20℃ to 23℃, which is within the ambient temperature as per the condition of local weather. Table 2 lists the thermo-physical properties of the used PCM such as density, thermal conductivity, and specific heat capacity.

One of the purposes of this study is to utilize nano-PCM in free cooling. Dispersing nanoparticles into the PCM is a complicated issue due to nanoparticles agglomeration; however, it can be solved by using functionalized nanoparticles. Thus, Multi-Wall Carbon Nanotube-Carboxyl (MWCNT-COOH) is considered as functionalized nanomaterials (diameter of < 8 nm, length of nearly 30 nm, purity of 95%, and density of 2.1 g/cm^3, US Research Nanomaterials Inc.) for the present research because of its high thermal conductivity. A carboxyl group (COOH) is a functional group consisting of a carbonyl group (C = O) with a hydroxyl group (O–H) attached to the same carbon atom. Table 1 summarizes some properties and features of the selected

Table 1
Selected nanoparticles (MWCNT-COOH).

Nanoparticles features	
Functional group	Carboxyl
Purity	95%
Effective area (m^2/g)	> 200
Length (μm)	5 – 10
diameter (nm)	20–30
Apparent density ($g.cm^{-3}$)	2.1

Table 2
PCM thermo-physical properties prepared by the manufacturer.

Thermal properties	
Specific heat capacity	2000 (J/(kg.K))
Melting range	20–23 (°C)
Heat storage capacity	190,000 (J/kg)
Heat conductivity (both phases)	0.2 (W/(m·K))
Density in liquid state at 50 °C	0.7 (kg/l)
Density in solid state at 20 °C	0.76 (kg/l)
Volume expansion	12.5 (%)
Flash point	>150 (°C)

nanoparticle. A TEM image of the mentioned nanoparticles is displayed in Fig. 1 [34]. These kinds of nano-sized particles have carboxyl group that helps the particles to disperse in the PCM better. So, functionalized nanoparticles are selected in nano-PCM construction process and the steps are depicted in Fig. 2. After purchasing these nanoparticles, they are added to the PCM with a certain weight fraction. Next, obtained mixture is stirred with 100 rpm speed and at 30C. Afterward, suspension is put in an ultrasonic bath (Elma, Elmasonic, S60H, and Germany) under sonication time of 30 min, a power of 400 W, with a frequency of 37 kHz, and a bath temperature of 40C. Finally, the stable nano-PCM is obtained. Four different weight fractions are examined for the present study (0%, 0.1%, 0.2%, and 0.5%) using the mentioned technique.

Thermal energy storage capacity and phase-change temperatures

In our previous work [34], which was focused on investigating the PCM and nano-PCM behavior during melting and solidification processes, the latent heat of fusion and thermal conductivity for both solid and liquid phases were measured. The samples were pure paraffin and nano-PCMs of 0.2 and 0.5 wt%. The data are presented in Table 3.

Due to low thermal conductivity of PCM, the addition of MWCNT nanoparticles to the PCM is proposed [35,36]. Addition of these particles has a marked effect on the thermal conductivity of the PCM so that the more the MWCNT nano-PCMs weight fraction, the higher the thermal conductivity of the sample. Thermal conductivity improvements of 45.4% and 49.3% in the liquid and solid phases are observed using 0.5 wt% nano-PCM. Besides, for 0.2 wt% nano-PCM in liquid and solid phases, the thermal conductivity increases approximately 18.94% and 35.29%, respectively [34].

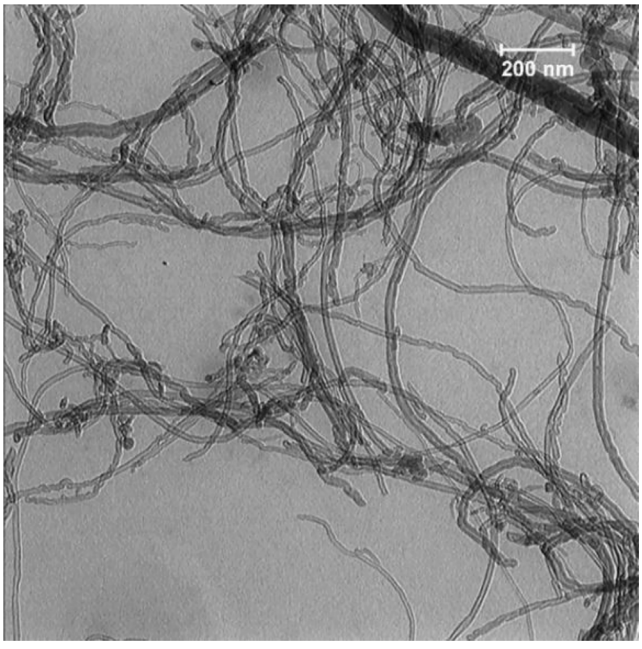

Fig. 1. TEM image of MWCNT nanoparticles [34].

Experimental setup

The experimental setup employed is an open air circuit, with an axial fan to move the air. A cooling and heating unit device are used to provide air with a specific temperature. Heating and cooling units contain heater elements and compression refrigeration cycle, respectively, in order to prepare warm and cold air. In the thermal energy storage there are various options for the PCM encapsulation geometry and the PCM heat exchanger. In the current work, selecting a shell and tubes heat exchanger is considered (Fig. 3b). The tubes are flat plate closures made of aluminum (high thermal conductivity) to observe the effect of temperature changes in air and PCMs. These closures are called PCM encapsulations that contain PCM inside. Each encapsulation has a dimension of 15 × 15 × 2 cm. Employing flat plate encapsulations provides an easy design of the thermal energy storage. The shell is a container with a dimension of 65 × 18 × 25 cm. Further, the shell is made from plates of woods (with a thickness of 1.5 cm) cover with elastomeric insulation in order to minimize thermal losses. Fig. 3 shows the experimental setup of the current study.

An automatic temperature control system is employed to achieve a specific temperature during charging and discharging tests. This controller system contains a solid-state relay (SSR) which is connected to the heating and cooling unit, and a TC4Y temperature indicator. Whenever the thermocouple at the inlet needs higher temperature (for example 17C in discharging period), the indicator sends a signal to SSR and controls the electric current of heating unit which can provide the desired temperature. Likewise, this process is performed for cooling unit.

The PCM encapsulations are located parallel to the air flow so that the air can flow along the encapsulations. A 2 cm gap is considered between each two of them. As seen in Fig. 3c, the temperature of the air is measured at the inlet and outlet of the heat exchanger. Due to symmetric geometry of the heat exchanger, the PCM temperature is measured and logged just for encapsulations number 1, 2, and 3 using five calibrated DS18B20 thermocouples (they are located at the center of each encapsulation). A calibrated flow-meter (UT211B 60A Mini Clamp Meter) is used to measure the air flow velocity. Finally, all the measured data are assessed.

Measurements

In order to perform energy analysis, first, the heat exchanger is examined as a control volume. The rates of heat entering or exiting the control volume are indicated in Fig. 4a.

Writing the first law of thermodynamics for Fig. 4:

$$\dot{E}_{in} - \dot{E}_{out} = \dot{E}_{storage} \tag{1}$$

$$\dot{m}h_i - \dot{m}h_e - Q_{env} = Q_{PCM} \tag{2}$$

where $\dot{m}$ is the mass flow rate, h_i is the inlet enthalpy, h_e is the outlet enthalpy, Q_{env} is the heat loss of the closure emitted to the environment and Q_{PCM} is the heat absorbed by PCM (in melting process) from the air. Air velocity measured to calculate the mass flow rate is 3 m/s. The terms in mentioned equation (Eq. (2)) can be simplified as:

$$\dot{m}h_i - \dot{m}h_e = \dot{m}C_p(T_i - T_e) \tag{3}$$

$$Q_{env} = \frac{T_{inside} - T_{outside}}{R_{wall}} \tag{4}$$

$$R_{wall} = \frac{l_w}{k_w A_w} + \frac{l_i}{k_i A_i} \tag{5}$$

where C_p is the heat capacity of the air, T_i and T_e are the inlet and outlet

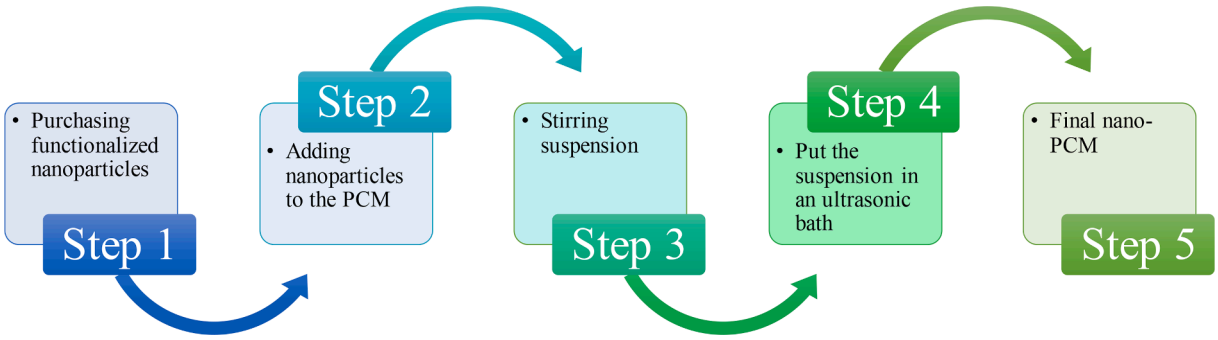

Fig. 2. Nano-PCM preparation steps.

Table 3
Latent heat of fusion and thermal conductivity in both liquid and solid phases [34].

Samples	Thermal conductivity (solid phase)	Thermal conductivity (liquid phase)	Latent heat of fusion kJ.kg^{-1}
Pure PCM	0.136	0.132	210
Nano-PCM 0.2 wt% MWCNT	0.184	0.157	184.3
Nano-PCM 0.5 wt% MWCNT	0.203	0.192	180.1

bulk temperatures, respectively, and T_{inside} and $T_{outside}$ are the inside and outside wall temperatures of the closure, respectively. R_{wall} is the overall resistance of the wall layers which is explained in terms of layer thickness l, the cross-section area A, and the thermal conductivity k. The mentioned heat values are then calculated for solidification process using the above relations and are summarized in Table 4. Finally, by substituting Eqs. (3) and (4) into Eq. (2) the Q_{PCM} is composed as:

$$Q_{PCM} = \dot{m}C_p(T_i - T_e) - \frac{T_{inside} - T_{outside}}{R_{wall}} \tag{6}$$

Uncertainty analysis

Uncertainty analysis of the experiments is done to authenticate the experimental results with considering the method presented in the literature [37]. The temperature thermocouples accuracy is considered to be ± 0.2 ℃ within the studied range. In order to ensure the data repeatability, some experiments are repeated at least three times. Parameter υ expresses the total uncertainty [38]:

$$\delta\nu_{tot} = \sqrt{(\delta\nu_{eqp})^2 + (\delta\nu_{rep})^2} \tag{7}$$

here $\delta\nu_{rep}$ and $\delta\nu_{eqp}$ are known as the repetition of uncertainty and the equipment uncertainty, respectively. If R is a function of some independent linear parameters (n), the uncertainty of R is calculated as:

$$\partial R = \sqrt{\left(\frac{\partial R}{\partial \nu_1}\delta\nu_1\right)^2 + \left(\frac{\partial R}{\partial \nu_2}\delta\nu_2\right)^2 + \ldots + \left(\frac{\partial R}{\partial \nu_n}\delta\nu_n\right)^2} \tag{8}$$

where the parameters are defined as: δR is the uncertainty of function R, $\delta\nu_i$ as the uncertainty of parameter ν_i, and $\partial R/\partial\nu_i$ as the partial derivative of R.

In this paper the total uncertainty of various parameters is reported in Table 5.

Result and discussion

The experimental tests using PCM and nano-PCM to fabricate an air-PCM heat exchanger are used in buildings in order to have an effective thermal management as well as enhanced energy performance. The early experimental tests are carried out to evaluate the thermocouples validation, performance, and comparison. Fig. 5 shows the temperature of the encapsulation #1, #2, and #3 for a charging test. Fig. 5 displays that all thermocouples measured approximately the same temperature. This fact implies that the heat exchanger is very well insulated. Therefore, reporting just one arbitrary encapsulation temperature instead of all three will not make a significant difference in the results.

Fig. 6 plots the weather conditions, including the ambient air temperature (inlet temperature), and solar radiation on horizontal surface for the three fall days (1 to 3 Nov. 2020) employed in this study. Based on Fig. 6 it can be found that the temperature of the ambient air (heat exchanger inlet temperature) only increased slightly after entering the heat exchanger and flowing through the PCM encapsulations. The maximum outlet air temperature of the heat exchanger under the experiment in the mentioned three days is 31.76 °C. During heating period the air is heated and flowed through the PCM encapsulations, therefore, the sun heat transferred into the PCM encapsulations through air. In contrast, during cooling period (night time), the air cooled and flowed among the encapsulations and the heat in the PCM units is discharged into the air.

Time-dependent temperature variations for the pure PCM encapsulation under both charging and discharging processes for four nanoparticles' concentrations (0%, 0.1%, 0.2%, 0.5%) are shown in Fig. 7 (experimental tests). From the results, it is observed that during melting process the temperature of the encapsulation increases concerning time due to heat supplied from the warm air. It is observed in Fig. 7 that increasing the inlet air temperature delayed meeting a determined set point temperature for both charging and discharging processes. When applying an air temperature of 29 °C, the PCM spends nearly 117.8 min in two-phase state while charging. Furthermore, increasing the air inlet temperature this time is postponed to almost 140.9 and 214 min for the air inlet temperatures of 27 and 25 °C, respectively. On the other hand, during discharging period, the case with the highest air inlet temperature (17 °C), stays at two-phase region for nearly 239.6 min. In contrast with melting process, reducing the air inlet temperature decreases the two-phase time, so that for cooling temperature of 15 and 13 °C this time becomes 231 and 201.1 min, respectively.

The influence of PCM mass fraction on the transient temperature of the encapsulation is non-linear because of various storage mechanisms and heat transfer modes like latent heating, sensible heating, conduction, and convection phenomenon as can be observed in Fig. 8. Six stages are considered for the system response. Sensible heating of system without melting is the first stage, where a steep rise of temperature is observed. Stage two commences as melting process begins. An apparent decline in the slope of temperature characterizes this stage. In addition, the temperature of the PCM cases in latent heating stage has a light rising trend as well as have a temperature near the melting point temperature; for example, After 200 min passes from the beginning, in this stage, the temperature of pure PCM and nano-PCMs 0.1%, 0.2% and 0.5% wt., are 22.25, 22.60, 22.92 and 23.20, respectively. As nano-PCM

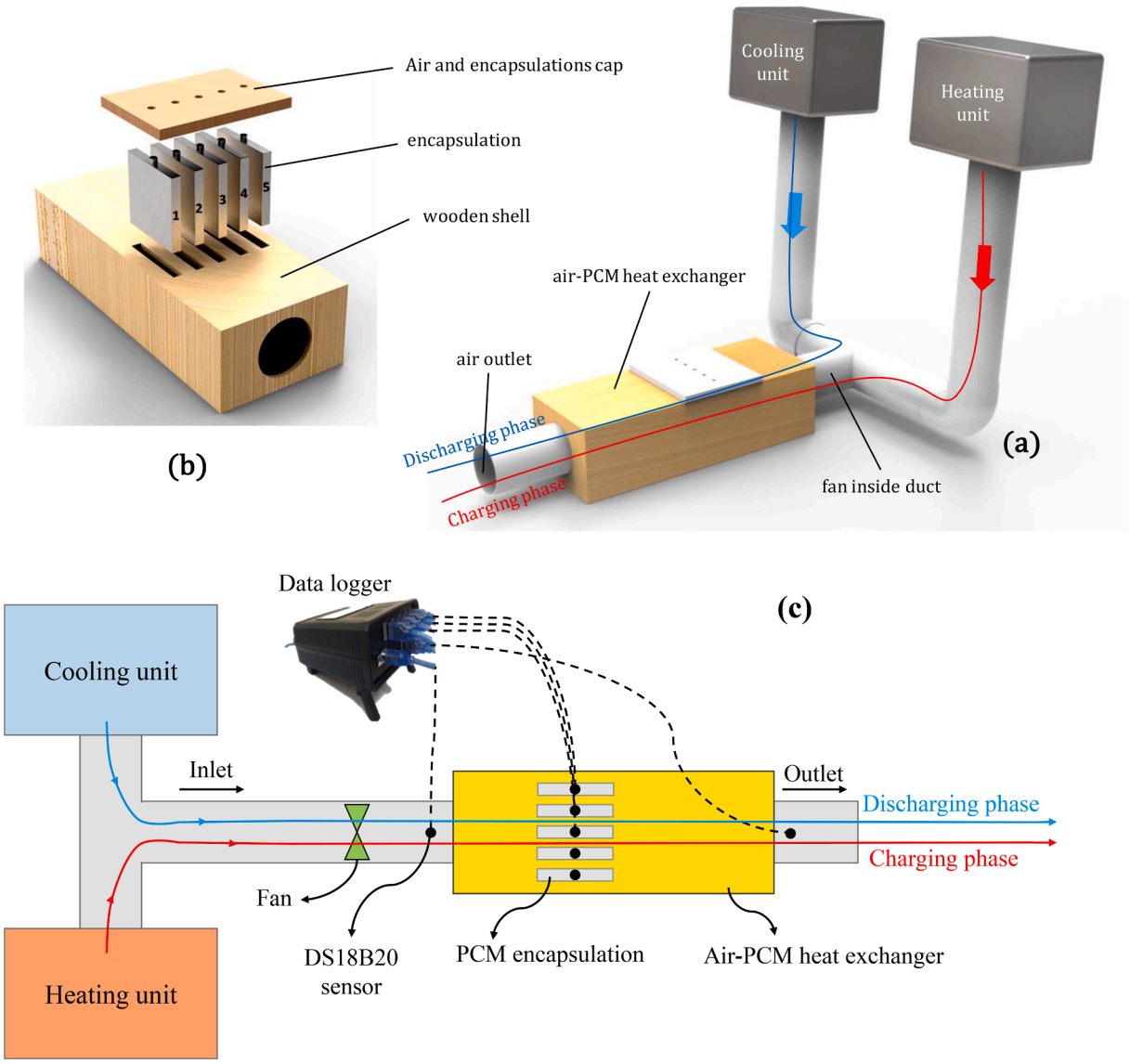

Fig. 3. a) 3D view of the Experimental setup, b) An exploded view of the heat exchanger and c) a schematic of the current experimental setup.

or pure PCM finishes melting process, Post-melting sensible heating stage begins. In this stage, there is a variation in encapsulation temperature. Next, a monotonic temperature increase in the encapsulation is achieved until getting to steady-state condition (25℃). Moreover, a similar period in encapsulation cooling can be observed. Sensible cooling is the fourth stage. After that, solidification period takes place where a change in temperature slope of the system exists. Finally, the last stage is post-sensible cooling where the temperature decreases smoothly to 17℃.

Furthermore, it is seen in the lab-scale results that using the nano-PCM augments the curve slope compared to employing pure PCM, demonstrating that the nano-PCM has higher solidification and melting rates, in comparison to that of the pure PCM. The rapid solidification rate during cooling period and the melting rate when heating is applied can increase the quantity of the heat discharged from or charged into the encapsulations per unit time.

Table 6 represents the air temperature difference between inlet and outlet sections as well as heat transfer rate of air flow while flowing through heat exchanger. These results report four types of PCMs (pure PCM and nano-PCMs) with the same inlet temperature of 25℃ during charging process. Meanwhile, it is indicated that the temperature difference for the case of nano-PCM is slightly higher than that the pure PCM during melting. Moreover, the addition of nanoparticles in the PCM causes higher air temperature difference and therefore enhancement of heat transfer rate is achieved compared to pure PCM. Two more quantities discussed in Table 5 are heat transfer rate and heat transfer improvement in comparison with pure PCM. Following the previous results about temperature differences, adding nano-powder MWCNT to the PCM leads to higher heat transfer rates. This parameter for pure PCM is 86.39 W and is enhanced up to 107.20 W in case of using nano-PCM 0.5% wt. It is worth mentioning that heat transfer rate increases slightly by increasing the nanoparticles concentration. 9.4%, 17.8%, and 24.1% more heat is charged into the heat exchanger that encapsulates nano-PCMs 0.1%, 0.2%, and 0.5% wt., respectively compared to the pure PCM. This enhancement is also observed qualitatively in the Fig. 8 by comparing the slope of the curves during melting. The higher the curve slope, the more the heat charged in the encapsulations.

Fig. 9 illustrates the mean temperature of nano-PCM 0.5% wt. and encapsulation wall in five different times which covers melting period for the encapsulation #3 (there is no difference between encapsulations temperature as stated before). Inside encapsulation (nano-PCM) temperature is measured by thermocouple sensor and the encapsulation outer wall temperature is quantified with the aid of a FLI0003- i5 Compact Infrared Thermal Imaging Camera. It can be seen, by the

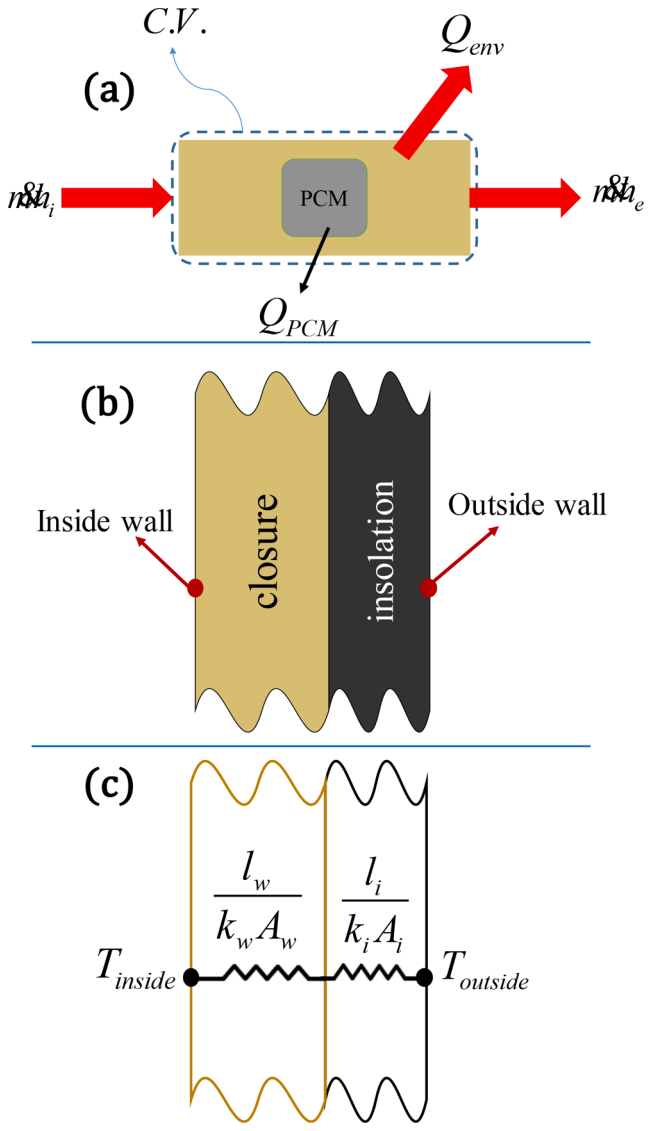

Fig. 4. a) a schematic of energy balance, b) shell construction, c) thermal resistance of the shell wall.

Table 4
Calculating the heat transfer rate for inlet, outlet, PCM, and heat loss.

Density	Heat of fusion	Q_{env}	Q_{out}	Q_{in}	Q_{PCM} (latent heat)
760 (kg/m^3)	53 (W/kg)	2.60 (W)	1217.05 (W)	1126.75 (W)	87.60 (W)

Table 5
Uncertainty of parameters in the experiments.

Equipment and model	Measurement section	Accuracy	Total uncertainty
DS18B20 thermocouple	Inlet temperature	±0.2 ℃	0.18℃
DS18B20 thermocouple	Outlet temperature	±0.2 ℃	0.21℃
DS18B20 thermocouple	Encapsulation temperature	±0.2 ℃	0.15℃

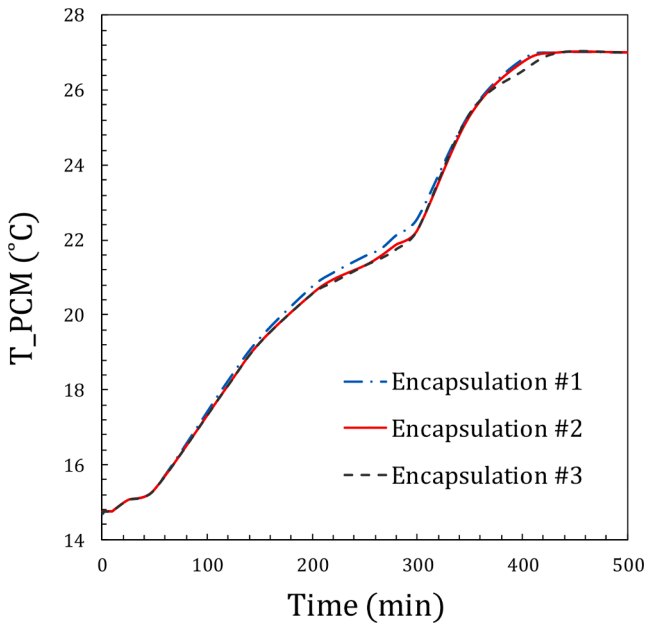

Fig. 5. Comparing the temperature of three encapsulations in a melting process.

change in color (temperature) of the capsule, that its wall has a nearly uniform temperature. Utilizing IR camera helped the authors to find out that during sensible heating (times a and e) the encapsulation wall temperature is near the nano-PCM temperature, whereas when latent heating this difference is much more. This phenomenon occurred because whenever the nano-PCM enters phase change region, the air heat is spent on changing phase of the nano-PCM, so its temperature rises more slowly than single-phase regions.

The cooling capacity and the performance of the encapsulations are carried out when the cooling unit turns on and the temperature controller (inlet temperature) is set at 13, 15, and 17 °C. Fig. 10 displays the solidification for four different types of PCM (pure PCM, nano-PCM with 0.1%, 0.2%, and 0.5% wt.). Fig. 10a depicts the time–temperature behavior when the inlet temperature is 13 °C and Fig. 10b is for 15 °C. In both figures the encapsulation temperature takes to fall from 25 °C to inlet temperature. Another point that could be discussed is the two-phase time. Rising the inlet temperature delays the two-phase time and let the PCM/nano-PCM discharge more heat into the air inside the heat exchanger. Besides, during solidification of the PCMs, adding nanoparticles to the PCM and increasing its concentration helps the nano-PCM to transfer more heat from encapsulation to the air (steeper slope of the nano-PCM curve compared to pure PCM curve when sensible cooling) at the same temperature. That's because of the high thermal conductivity of the MWCNT nanoparticles compared to pure PCM. The case with an inlet temperature of 17 °C was expressed in Fig. 8.

Conclusions and future research

Conclusions

In present work an air-PCM heat exchanger containing five similar PCM encapsulations that could be applied in buildings was proposed in order to have an influential thermal management as well as enhanced energy performance. The following items are the main points of this section:

- It can be stated that the temperature of the ambient warm air (during daytime) after entering the heat exchanger and flowing through the PCM encapsulations (congealed previous night) decreased slightly.

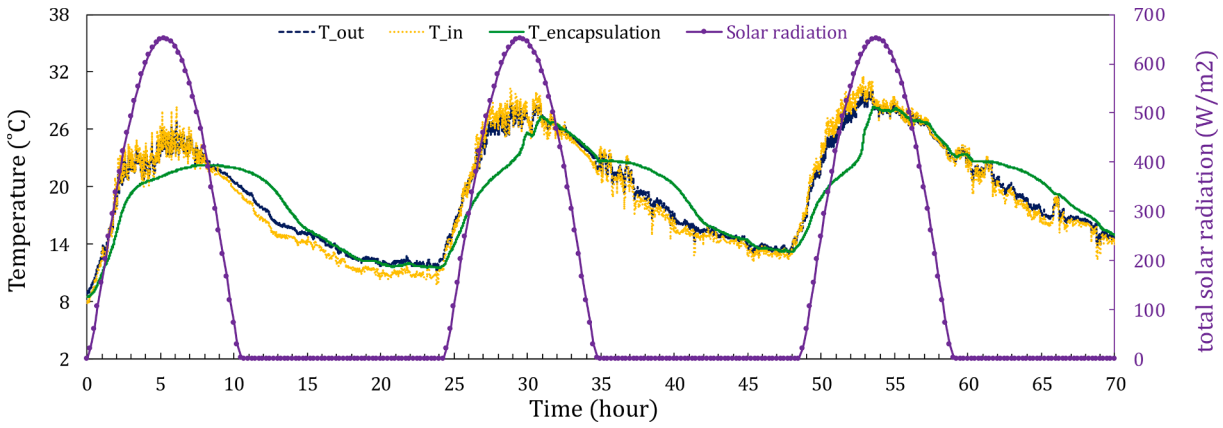

Fig. 6. Solar radiation, inlet and outlet temperature, and encapsulations temperature under three successive winter days.

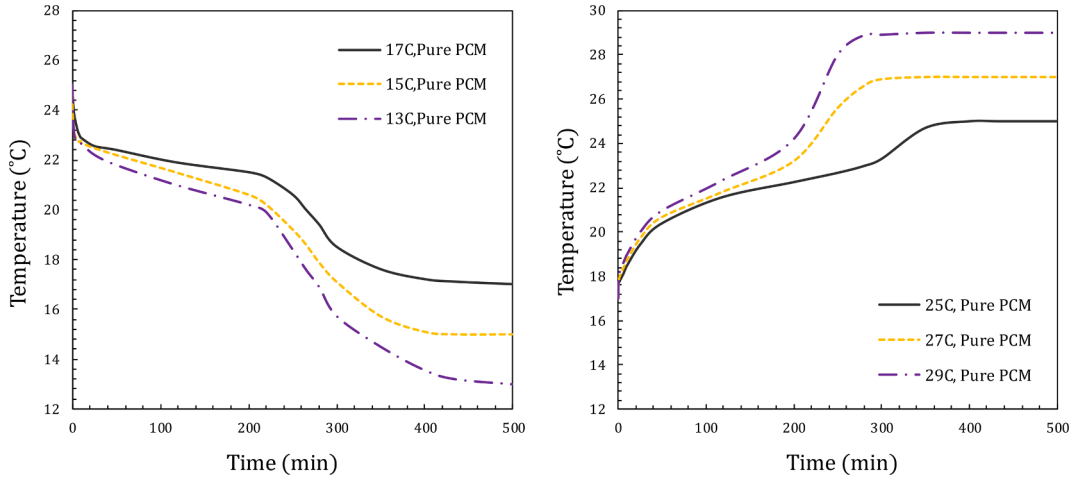

Fig. 7. Time- temperature behavior of the PCM with variation of inlet temperature.

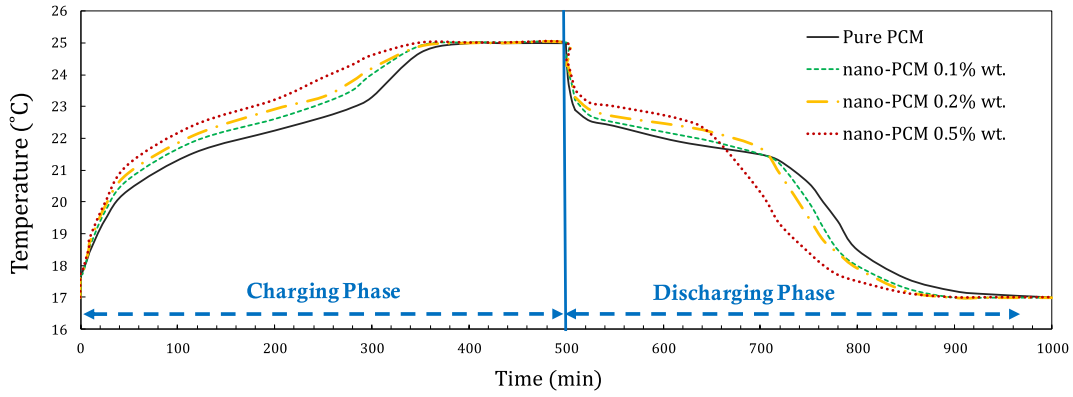

Fig. 8. Time temperature behavior of the pure PCM and nano-PCM (3 concentrations) during charging and discharging periods; melting: inlet temperature of 25C, solidification: inlet temperature of 17C.

Table 6
Air temperature difference between inlet and outlet, heat absorbed by air, and heat transfer improvement.

Type	T_{out}-T_{in}	q (W)	% improvement q
Pure PCM	1.91	86.39	–
nano-PCM 0.1% wt.	2.09	94.54	9.4
nano-PCM 0.2% wt.	2.25	101.78	17.8
nano-PCM 0.5% wt.	2.37	107.20	24.1

During three days tests, the maximum outlet air temperature of the heat exchanger was 31.76 °C.

- Increasing the air inlet temperature delayed meeting a determined set point temperature for both charging and discharging processes.
- The two-phase time reduced as the air inlet temperature reduces when cooling period or the air inlet temperature increases when heating process.
- Addition of nano-powder MWCNT to the PCM led to a higher heat transfer rate. This parameter for pure PCM was 86.39 W and was

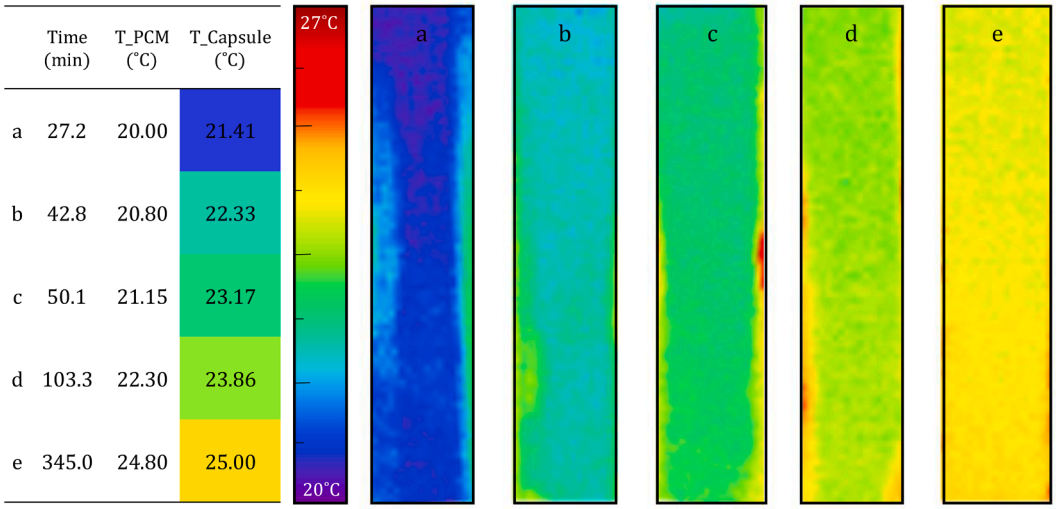

Fig. 9. Temperature of nano-PCM 0.5% wt. and encapsulation wall at five different times cover melting period (25C).

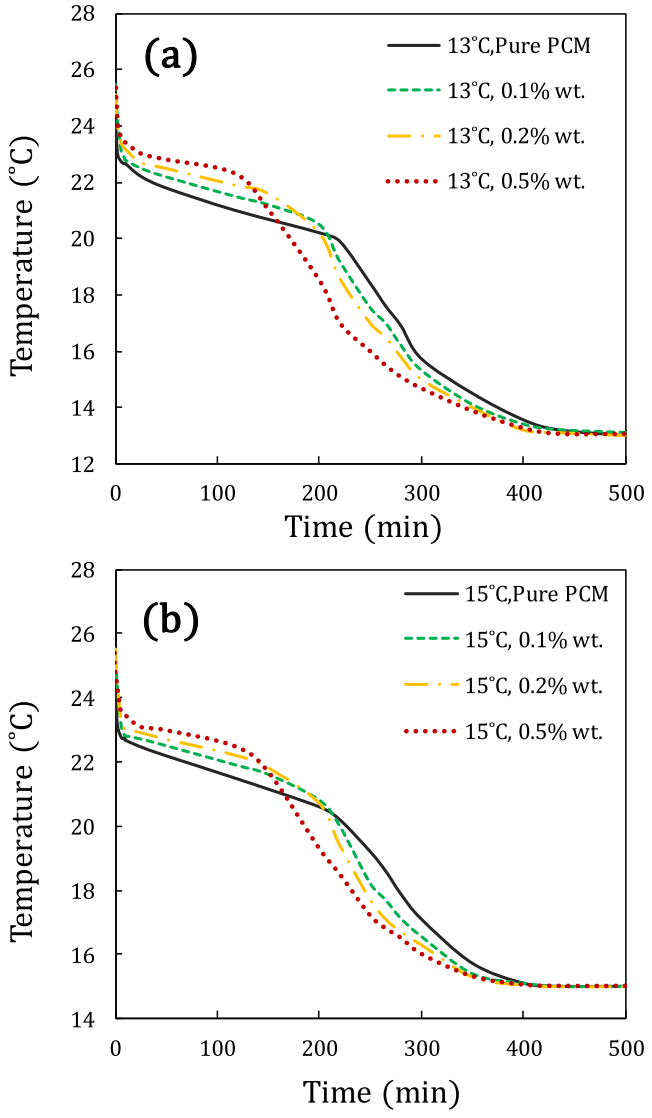

Fig. 10. Time-temperature behavior of the four types of PCM during solidifications with inlet temperature of a) 13C, and b) 15C.

improved up to 107.20 W in case of utilizing nano-PCM 0.5% wt. This illustrated 24.1% enhancement in heat transfer rate.

- Employing IR camera aided the authors to realize that during sensible heating the encapsulations wall temperature was near the nano-PCM temperature (@T_{PCM} = 20.00: $T_{encapsulation}$ = 21.41; whereas during latent heating, this difference was much more (@ T_{PCM} = 21.15: $T_{encapsulation}$ = 23.17;). This phenomenon was occurred because whenever the nano-PCM entered phase change region, the air heat was spent on changing phase of the nano-PCM, so its temperature rose more slowly than sensible heating regions.

Future research:

- Investigating air-PCM heat exchanger using other PCMs with different properties.
- Changing the encapsulations geometry and its effect on the heat exchanger performance.
- Effect of adding other metallic and non-metallic nanopowders to PCM on the heat exchanger performance.
- Experimental tests in an actual room considered for future works.

CRediT authorship contribution statement

Mahdi Kazemi: Formal analysis, Writing – original draft. **Ali Kianifar:** Writing – original draft, Supervision, Conceptualization. **Hamid Niazmand:** Writing – original draft, Supervision, Conceptualization.

Declaration of Competing Interest

The authors declare that they have no known competing financial interests or personal relationships that could have appeared to influence the work reported in this paper.

References

[1] Bölük G, Mert MJE. Fossil & renewable energy consumption, GHGs (greenhouse gases) and economic growth: Evidence from a panel of EU (European Union) countries. 2014;74:439-46.
[2] Park S, Pandey A, Tyagi V, Tyagi SJR, Reviews SE. In: Energy and exergy analysis of typical renewable energy systems; 2014. p. 105–23.
[3] Seddegh S, Wang X, Henderson AD, Xing Z. In: reviews Se. Solar domestic hot water systems using latent heat energy storage medium: a review; 2015. p. 517–33.
[4] Sharma RK, Ganesan P, Tyagi VV, Metselaar HSC, Sandaran SC. In: Thermal properties and heat storage analysis of palmitic acid-TiO2 composite as nano-enhanced organic phase change material (NEOPCM); 2016. p. 1254–62.

[5] Arshad A, Ali HM, Khushnood S, Jabbal M. Experimental investigation of PCM based round pin-fin heat sinks for thermal management of electronics: effect of pin-fin diameter. Int J Heat Mass Transf 2018;117:861–72.
[6] Farzanehnia A, Khatibi M, Sardarabadi M, Passandideh-Fard M. Experimental investigation of multiwall carbon nanotube/paraffin based heat sink for electronic device thermal management. Energy Convers Manage 2019;179:314–25.
[7] Liao X, Liu Y, Ren J, Guan L, Sang X, Wang B, et al. Investigation of a double-PCM-based thermoelectric energy-harvesting device using temperature fluctuations in an ambient environment. Energy 2020;202:117724. https://doi.org/10.1016/j.energy.2020.117724.
[8] Sivashankar M, Selvam C, Manikandan S, Harish S. Performance improvement in concentrated photovoltaics using nano-enhanced phase change material with graphene nanoplatelets. Energy 2020;208:118408. https://doi.org/10.1016/j.energy.2020.118408.
[9] Chopra K, Tyagi VV, Pandey AK, Sharma RK, Sari A. PCM integrated glass in glass tube solar collector for low and medium temperature applications: Thermodynamic & techno-economic approach. Energy 2020;198:117238.
[10] Yousef MS, Hassan H. Energetic and exergetic performance assessment of the inclusion of phase change materials (PCM) in a solar distillation system. Energy Convers Manage 2019;179:349–61.
[11] Nasef HA, Nada SA, Hassan H. Integrative passive and active cooling system using PCM and nanofluid for thermal regulation of concentrated photovoltaic solar cells. Energy Convers Manage 2019;199:112065. https://doi.org/10.1016/j.enconman.2019.112065.
[12] Sheikholeslami M, Jafaryar M, Shafee A, Babazadeh H. Acceleration of discharge process of clean energy storage unit with insertion of porous foam considering nanoparticle enhanced paraffin. J Cleaner Prod 2020;261:121206. https://doi.org/10.1016/j.jclepro.2020.121206.
[13] Mukhamet T, Kobeyev S, Nadeem A, Memon SA. Ranking PCMs for building façade applications using multi-criteria decision-making tools combined with energy simulations. Energy 2021;215:119102. https://doi.org/10.1016/j.energy.2020.119102.
[14] Rostami S, Afrand M, Shahsavar A, Sheikholeslami M, Kalbasi R, Aghakhani S, et al. A review of melting and freezing processes of PCM/nano-PCM and their application in energy storage. Energy 2020;211:118698. https://doi.org/10.1016/j.energy.2020.118698.
[15] Diallo TMO, Yu M, Zhou J, Zhao X, Shittu S, Li G, et al. Energy performance analysis of a novel solar PVT loop heat pipe employing a microchannel heat pipe evaporator and a PCM triple heat exchanger. Energy 2019;167:866–88.
[16] Zhu Na, Li S, Hu P, Lei F, Deng R. Numerical investigations on performance of phase change material Trombe wall in building. Energy 2019;187:116057. https://doi.org/10.1016/j.energy.2019.116057.
[17] Liu L, Li J, Niu J, Wu J-Y. Evaluation of the energy storage performance of PCM nano-emulsion in a small tubular heat exchanger. Case Stud Therm Eng. 2021;26:101156. https://doi.org/10.1016/j.csite.2021.101156.
[18] Liu Y, Wang M, Cui H, Yang L, Liu J. In: Micro-/macro-level optimization of phase change material panel in building envelope; 2020. p. 116932. https://doi.org/10.1016/j.energy.2020.116932.
[19] Zalba B, Marín JM, Cabeza LF, Mehling H. Free-cooling of buildings with phase change materials. Int J Refrig 2004;27(8):839–49.
[20] Pandey A, Hossain M, Tyagi V, Rahim NA, Jeyraj A, Selvaraj L, et al. Novel approaches and recent developments on potential applications of phase change materials in solar energy. Renew Sustain Energy Rev 2018;82:281–323.
[21] Kasaeian A, bahrami L, Pourfayaz F, Khodabandeh E, Yan W-M. Experimental studies on the applications of PCMs and nano-PCMs in buildings: A critical review. Energy Build 2017;154:96–112.
[22] Wu S, Zhu D, Zhang X, Huang J. Preparation and melting/freezing characteristics of Cu/paraffin nanofluid as phase-change material (PCM). Energy Fuels 2010;24(3):1894–8.
[23] Iten M, Liu S, Shukla AJR, Reviews SE. In: A review on the air-PCM-TES application for free cooling and heating in the buildings; 2016. p. 175–86.
[24] Gholamibozanjani G, Farid M. In: Application of an active PCM storage system into a building for heating/cooling load reduction; 2020. p. 118572. https://doi.org/10.1016/j.energy.2020.118572.
[25] Castell A, Belusko M, Bruno F, Cabeza LF. Maximisation of heat transfer in a coil in tank PCM cold storage system. Appl Energy 2011;88(11):4120–7.
[26] Ravikumar M, Srinivasan PJJoT, Technology AI. Phase Change Material as a thermal energy storage material for cooling of building. 2008;4(6).
[27] Mishra AK, Lahiri BB, Philip J. In: Carbon black nano particle loaded lauric acid-based form-stable phase change material with enhanced thermal conductivity and photo-thermal conversion for thermal energy storage; 2020. p. 116572. https://doi.org/10.1016/j.energy.2019.116572.
[28] Kabeel A, Sathyamurthy R, Manokar AM, Sharshir SW, Essa F, Elshiekh AHJJoES. Experimental study on tubular solar still using Graphene Oxide Nano particles in Phase Change Material (NPCM's) for fresh water production. 2020;28:101204.
[29] Rathore PKS, Shukla SK. Improvement in thermal properties of PCM/Expanded vermiculite/expanded graphite shape stabilized composite PCM for building energy applications. Renew Energy 2021;176:295–304.
[30] Sheikholeslami M, Mahian OJJocp. Enhancement of PCM solidification using inorganic nanoparticles and an external magnetic field with application in energy storage systems. 2019;215:963-77.
[31] Santos T, Kolokotroni M, Hopper N, Yearley KJEP. Experimental study on the performance of a new encapsulation panel for PCM's to be used in the PCM-Air heat exchanger. 2019;161:352-9.
[32] Kant K, Pitchumani R, Shukla A, Sharma AJEC, Management. Analysis and design of air ventilated building integrated photovoltaic (BIPV) system incorporating phase change materials. 2019;196:149-64.
[33] Ousegui A, Marcos B, Havet MJATE. Inverse method to estimate air flow rate during free cooling using PCM-air heat exchanger. 2019;146:432-9.
[34] Kazemi M, Kianifar A, Niazmand HJJoTA, Calorimetry. Nanoparticle loading effect on the performance of the paraffin thermal energy storage material for building applications. 2020;139(6):3769-75.
[35] Khatibi M, Nemati-Farouji R, Taheri A, Kazemian A, Ma T, Niazmand H. Optimization and performance investigation of the solidification behavior of nano-enhanced phase change materials in triplex-tube and shell-and-tube energy storage units. J Storage Mater 2021;33:102055. https://doi.org/10.1016/j.est.2020.102055.
[36] Entezari S, Taheri A, Khatibi M, Niazmand H. Acceleration of melting process of phase change material using an innovative triplex-tube helical-coil storage unit: Three-dimensional numerical study. J Storage Mater 2021;39:102603. https://doi.org/10.1016/j.est.2021.102603.
[37] Sivashankar M, Selvam C, Manikandan S, Harish SJE. Performance improvement in concentrated photovoltaics using nano-enhanced phase change material with graphene nanoplatelets. 2020;208:118408.
[38] Sardarabadi M, Passandideh-Fard MJSEM, Cells S. Experimental and numerical study of metal-oxides/water nanofluids as coolant in photovoltaic thermal systems (PVT). 2016;157:533-42.